

# The Injected Dark Current of a $p^+n$ and a $p^+n n^+$ Silicon Solar Cell Taking into Account the Narrowing of Band Gap Due to Heavy Doping

Ashim Kumar Biswas\*, Sayantan Biswas\*, Avigyan Chatterjee\* and Amitabha Sinha\*<sup>‡</sup>

\*Department of Physics, University of Kalyani, Kalyani-741235, West Bengal, India.

(kumarashimbiswas@gmail.com, sayan.solar@gmail.com, avigyan.chatterjee@gmail.com, asinha333@gmail.com)

<sup>‡</sup>Corresponding Author; Amitabha Sinha, Department of Physics, University of Kalyani, Kalyani-741235, West Bengal, India.  
Tel: +919330951068, asinha333@gmail.com

*Received: 12.08.2015 Accepted:02.10.2015*

**Abstract-** In addition to the photocurrent, the dark current of solar cell plays a vital role in determining the overall efficiency of a solar cell. In this paper, the injected dark current of a  $p^+n$  junction solar cell and that of a  $p^+n n^+$  back-surface-field cell have been studied analytically, taking into account the band gap narrowing effect that exists at high doping concentrations. It is observed that there is a significant difference in the magnitude of the injected dark current obtained when the band gap narrowing effect is taken into consideration as compared to the case when it is not considered. Also, it is observed that the magnitude of the injected dark current decreases for smaller values of back surface recombination velocity, which corresponds to BSF structure. This is one of the reasons why the  $p^+n n^+$  BSF solar cell has better output than the conventional  $p^+n$  cell. The results obtained here are similar to the case of an  $n^+p p^+$  solar cell reported earlier by researchers.

**Keywords-** Injected dark current, band gap narrowing, effective back surface recombination velocity, solar cells.

## 1. Introduction

Ever since the development of the first silicon solar cell [1], tremendous amount of research and development work has been done to improve the efficiency of these cells [2-5]. A back-surface-field (BSF) silicon solar cell was first reported by Mandelkorn et al. [6] which showed much improved efficiency over conventional solar cells. In the BSF solar cell, a heavily doped layer was incorporated at the back of the normal solar cell, which led to much higher efficiency. Though lot of research work has been done on  $n^+pp^+$  solar cells, only a few papers appeared on  $p^+n n^+$  BSF solar cells [7-9]. Recently, analytical work on the minority carrier distribution and the spectral response of a  $p^+n n^+$  solar cell has been carried out [10] and the results have been compared with that of the conventional  $p^+n$  structure. In addition to the photocurrent, the dark current of a solar cell also plays a vital role in deciding the performance of a solar cell. The current passing through the load is the difference between the photocurrent and the dark current. Analytical formulation of the dark current of an  $n$  on  $p$  solar cell is available in standard text [11]. Recently, dark current-voltage characteristics and lock-in thermography techniques for

silicon solar cell has been discussed [12]. The intrinsic carrier concentration in the semiconductor is a function of temperature and increases as temperature rises [13]. As the doping concentration in the semiconductor increases, the intrinsic carrier concentration is not only a function of temperature, but also a function of impurity concentration [14]. In the BSF solar cell, there is a low – high junction and the effect of heavy doping on the properties of low – high junction has already been studied for a  $p p^+$  junction [15] and it has been observed that it changes the effective back surface recombination velocity. In our present paper, an analytical study has been carried out on the injected dark current of a  $p^+n n^+$  solar cell, with particular reference to  $p^+n n^+$  BSF structure. The low – high junction here consists of an  $n n^+$  junction. The analytical study has therefore taken into account this type of junction. Since band gap narrowing takes place in the heavily doped semiconductors [14], in the present analysis, the effect of heavy doping has also been considered. It may be mentioned here that the effect of back surface field on the photocurrent in a solar cell has already been studied [16], but not much work has been reported on the dark current. In this paper, therefore, a study on the injected dark current of the solar cell has been undertaken.

## 2. Analysis

The dimensions and structure of the solar cell considered for the analysis are shown in Fig.1.

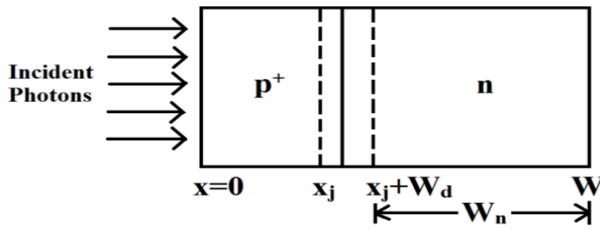


Fig. 1. A p<sup>+</sup> n junction solar cell.

In order to obtain the expressions for the excess minority carrier concentration and the injected dark current of a p<sup>+</sup> n junction silicon solar cell, the method described by Hovel [11] for the n<sup>+</sup> p solar cell, has been followed here. The behavior of the minority carriers is governed by the continuity equations

$$\frac{1}{q} \left( \frac{dJ_n}{dx} \right) - \left[ \frac{(n_p - n_{p0})}{\tau_n} \right] = 0 \quad (1)$$

(for electrons in the p - side)

$$\frac{1}{q} \left( \frac{dJ_p}{dx} \right) + \left[ \frac{(p_n - p_{n0})}{\tau_p} \right] = 0 \quad (2)$$

(for holes in the n - side)

where  $\tau_n$  and  $\tau_p$  are the electrons and holes life times respectively.

Since the solar cell considered here is of uniform doping in both sides of the junction, electric field outside the depletion region has been taken as negligible.

Hence the electron and hole current density equations are written as

$$J_n = qD_n \left( \frac{dn_p}{dx} \right) \quad (p - side) \quad (3)$$

$$J_p = -qD_p \left( \frac{dp_n}{dx} \right) \quad (n - side) \quad (4)$$

where  $D_n$  and  $D_p$  are the diffusion coefficients for electrons and holes respectively.

Using equation (3) in equation (1) and equation (4) in equation (2), the following equations are obtained.

$$\frac{d^2(n_p - n_{p0})}{dx^2} - \frac{1}{D_n \tau_n} (n_p - n_{p0}) = 0 \quad (5)$$

and

$$\frac{d^2(p_n - p_{n0})}{dx^2} - \frac{1}{D_p \tau_p} (p_n - p_{n0}) = 0 \quad (6)$$

These are the differential equations for the excess electron concentration in p- side and the excess hole concentration in n - side. The solutions of the above two differential equations are given respectively by [11]

$$n_p - n_{p0} = A_1 \cosh \left( \frac{x}{L_n} \right) + B_1 \sinh \left( \frac{x}{L_n} \right) \quad (for \ x \leq x_j) \quad (7)$$

and

$$p_n - p_{n0} = A_2 \cosh \left[ \frac{x - (x_j + W_d)}{L_n} \right] + B_2 \sinh \left[ \frac{x - (x_j + W_d)}{L_n} \right] \quad (for \ (x_j + W_d) \leq x \leq W) \quad (8)$$

where  $L_n = (D_n \tau_n)^{1/2}$  and  $L_p = (D_p \tau_p)^{1/2}$  are respectively the diffusion lengths for electrons and for holes,  $A_1$ ,  $B_1$ ,  $A_2$  and  $B_2$  are the four constants which may be evaluated using the following boundary conditions.

$$1. \text{ At } x = 0, \quad S_n (n_p - n_{p0}) = D_n \frac{d(n_p - n_{p0})}{dx} \quad (9)$$

$$2. \text{ At } x = x_j, \quad n_p = n_{p0} \exp \left( \frac{qV_j}{kT} \right) \quad (10)$$

$$3. \text{ At } x = x_j + W_d, \quad p_n = p_{n0} \exp \left( \frac{qV_j}{kT} \right) \quad (11)$$

where  $V_j$  is the light generated junction potential across the junction.

4. At the end of the cell, that is at  $x = W$ ,

$$S_p (p_n - p_{n0}) = -D_p \frac{d(p_n - p_{n0})}{dx} \quad (12)$$

Putting the calculated values of the said constants in the respective equations (7) and (8), the expressions for the excess minority carrier concentrations are given by

$$n_p - n_{p0} = \frac{n_i^2 \left[ \exp \left( \frac{qV_j}{kT} \right) - 1 \right]}{N_a} \times \frac{\left[ \frac{S_n L_n}{D_n} \sinh \left( \frac{x}{L_n} \right) + \cosh \left( \frac{x}{L_n} \right) \right]}{\left[ \frac{S_n L_n}{D_n} \sinh \left( \frac{x_j}{L_n} \right) + \cosh \left( \frac{x_j}{L_n} \right) \right]} \quad (13)$$

where  $n_{p0} N_a \approx n_i^2$  and  $n_i$  is the intrinsic carrier concentration.

$$p_n - p_{n0} = \frac{n_i^2 \left[ \exp \left( \frac{qV_j}{kT} \right) - 1 \right]}{N_d} \times \left[ \cosh \left( \frac{x - (x_j + W_d)}{L_p} \right) - \frac{\frac{S_p L_p}{D_p} \cosh \left( \frac{W_n}{L_p} \right) + \sinh \left( \frac{W_n}{L_p} \right)}{\frac{S_p L_p}{D_p} \sinh \left( \frac{W_n}{L_p} \right) + \cosh \left( \frac{W_n}{L_p} \right)} \times \sinh \left( \frac{x - (x_j + W_d)}{L_p} \right) \right] \quad (14)$$

where  $p_{n0} N_d \approx n_i^2$  and  $W_n = W - (x_j + W_d)$ , and  $W_d$  is the depletion width.

The final expression for the injected dark current is thus obtained as [11]

$$J_{inj} = J_0 \left[ \exp \left( \frac{qV_j}{kT} \right) - 1 \right] \quad (15)$$

where  $J_o$  is the injected dark current component which is given by [11]

$$J_o = q \frac{D_n n_i^2}{L_n N_a} \left[ \frac{\frac{S_n L_n}{D_n} \cosh\left(\frac{x_j}{L_n}\right) + \sinh\left(\frac{x_j}{L_n}\right)}{\frac{S_n L_n}{D_n} \sinh\left(\frac{x_j}{L_n}\right) + \cosh\left(\frac{x_j}{L_n}\right)} \right] + q \frac{D_p n_i^2}{L_p N_d} \left[ \frac{\frac{S_p L_p}{D_p} \cosh\left(\frac{W_n}{L_p}\right) + \sinh\left(\frac{W_n}{L_p}\right)}{\frac{S_p L_p}{D_p} \sinh\left(\frac{W_n}{L_p}\right) + \cosh\left(\frac{W_n}{L_p}\right)} \right] \quad (16)$$

For higher impurity concentration, the intrinsic carrier concentration  $n_i$  depends on temperature as well as impurity concentration according to the relation given by Slotboom [14] which is

$$n_{ie}^2(N, T) = n_i^2(T) \exp\left(\frac{q\Delta V_{go}(N)}{kT}\right) \quad (17)$$

where  $n_{ie}$  is the effective intrinsic carrier concentration and  $n_i(T)$  is given by the relation[14]

$$n_i^2(T) = CT^3 \exp\left(-\frac{1.206}{kT}\right) \quad (18)$$

where  $C = 9.61 \times 10^{32} \text{ cm}^{-6} \text{ K}^{-3}$  for silicon.

Band gap narrowing,  $\Delta V_{go}$  in equation (17) for p-type and n-type silicon has been respectively calculated from the formula discussed by A.W. Wieder [17] and Slotboom [14].

We now consider a  $p^+n^+$  back-surface-field structure. Dimensions and structure of the solar cell considered for analysis are shown in Fig.2.

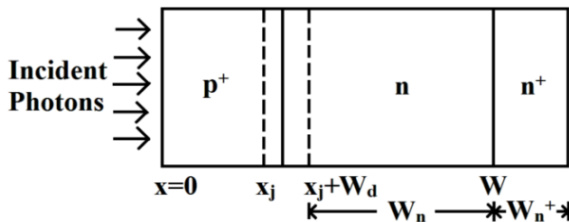


Fig. 2. A  $p^+n^+$  BSF solar cell.

When an  $n^+$  layer is present at the back of a normal  $p^+$  structure, an effective back surface recombination velocity seen by the holes in the  $n$  region will be  $S$  instead of  $S_p$ , as shown Godlewski et al. [4]

$$S = \frac{N_d D_p^+}{N_d^+ L_p^+} \left[ \frac{\frac{S_p L_p^+}{D_p^+} \cosh\left(\frac{W_n^+}{L_p^+}\right) + \sinh\left(\frac{W_n^+}{L_p^+}\right)}{\frac{S_p L_p^+}{D_p^+} \sinh\left(\frac{W_n^+}{L_p^+}\right) + \cosh\left(\frac{W_n^+}{L_p^+}\right)} \right] \quad (19)$$

Substituting this value of  $S$  in equation (16), the expression of  $J_o$  for a BSF solar cell may be obtained.

Here  $N_d, D_p, L_p$  are the values of donor concentration, diffusion constant for holes and diffusion length for holes in the  $n$ -type base region, while  $N_d^+, D_p^+, L_p^+$  are the corresponding values for the  $n^+$  region.  $W_n$  and  $W_n^+$  are the widths of the lightly and heavily doped base regions, respectively.

### 3. Results and discussion

Calculations have been done to obtain the values of different device parameters as discussed here. The depletion width,  $W_d$ , has been calculated following Sze [18]. The doping dependent mobilities and hence the diffusion coefficients for minority carriers (electrons and holes) in the respective regions have been taken from the published literature [19] and the doping dependent minority carrier life time and hence diffusion length have been evaluated by [20].

Fig.3 shows the plot of minority carrier concentration as a function of distance  $x$  from the junction edge into the base region of the cell. The dotted line is for the cases when heavy doping effect are not considered and the solid line is the case when heavy doping effect has been taken into account. The minority carrier density falls near the back surface because of recombination at the back of the cell.

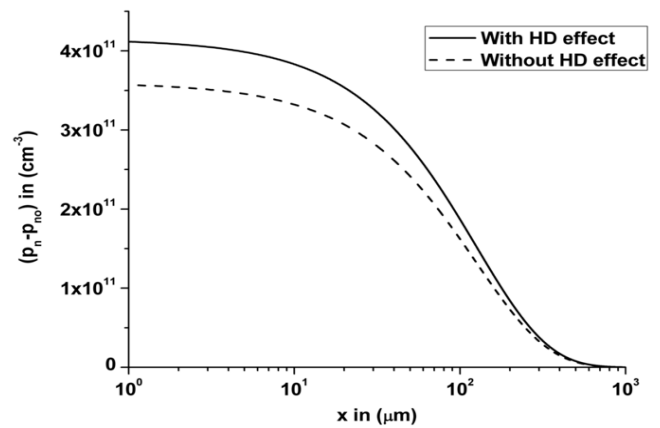


Fig. 3. Minority carrier concentration as a function of distance  $x$  from the junction edge into the base region of the cell.

The injected dark current ( $J_{inj}$ ) against junction depth ( $x_j$ ) has been plotted in Fig.4. The solid curve corresponds to the case when heavy doping effect is considered and the dotted curve corresponds to the case when heavy doping effect is not considered. The difference in the injected dark current in the two curves is created due to band gap narrowing effect when doping concentration becomes high.

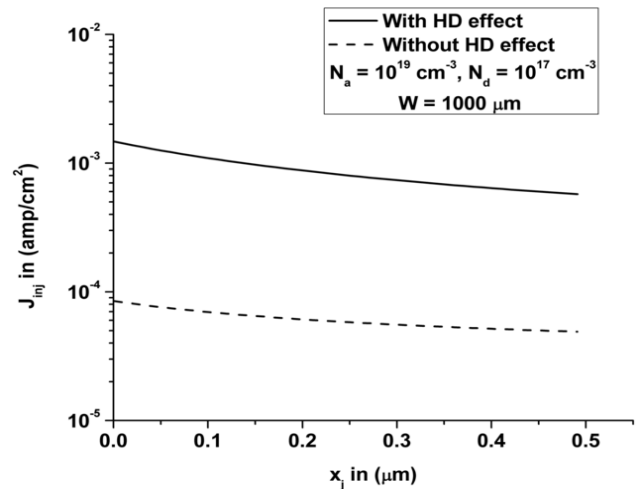
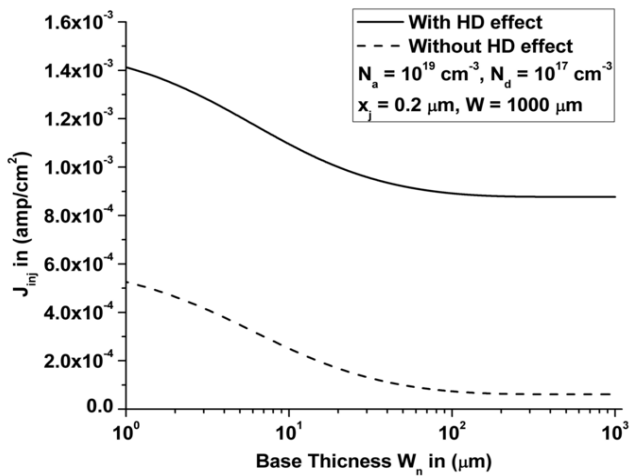


Fig. 4. Injected dark current ( $J_{inj}$ ) versus junction depth ( $x_j$ ).

The variation of injected dark current with base thickness of the cell has been shown in fig.5. Injected dark

current gradually decreases as base thickness is increased but after reaching a certain value, it becomes almost independent of the base thickness. The difference in the dark current observed in the two curves is due to the effect of the band gap narrowing.



**Fig. 5.** Injected dark current ( $J_{inj}$ ) versus base thickness ( $W_n$ ) of the cell.

The injected dark current  $J_{inj}$  as a function of donor concentration  $N_d$  has been plotted in Fig. 6 for different values of effective back surface recombination velocity  $S$ . Different curves in this graph shows that as  $S$  increases, injected dark current  $J_{inj}$  also increases. On the other hand for a particular value of  $S$ , as donor concentration in the base region gradually increases,  $J_{inj}$  decreases. It is also observed that after reaching a certain value of  $N_d$ ,  $J_{inj}$  becomes independent of the value of  $S$ .

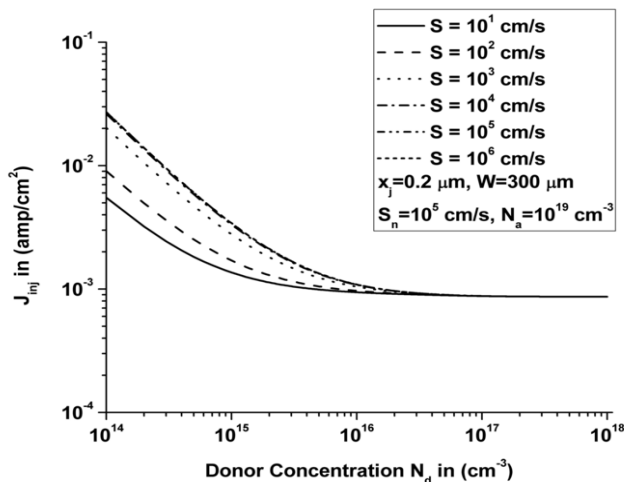


**Fig. 6.** Injected dark current ( $J_{inj}$ ) versus donor concentration ( $N_d$ ) for various values of effective back surface recombination velocity.

In Fig.7 the effective back surface recombination velocity  $S$  has been plotted against  $W_n^+$ , for different values of donor concentration in the heavily doped region. The value of  $S_p$  has been taken as  $10^5$  cm/sec for this graph. The calculations have been performed based on equation (19) which has been derived by Godlewski [4]. When donor

concentration in the  $n^+$  region increases, the effective back surface recombination velocity decreases, which is the expected result. This may be interpreted in this way that for higher doping, the BSF effect becomes greater, resulting in little recombination and hence the small recombination velocity. On the other hand for the particular values of  $N_d^+$  when  $W_n^+$  increases,  $S$  initially remains nearly constant and then decreases as the width  $W_n^+$  is further increased.

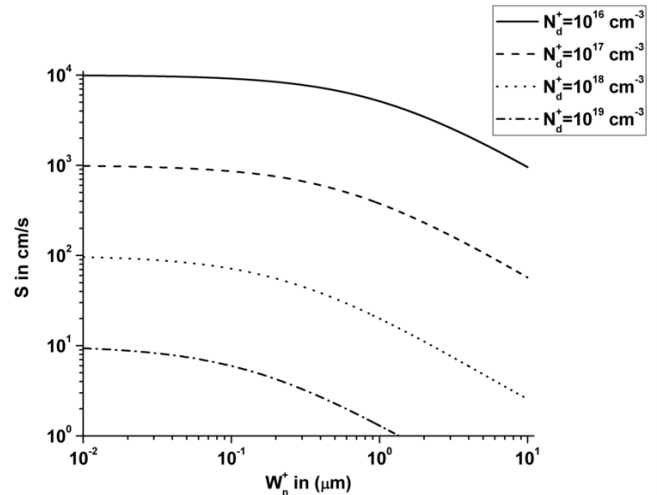


**Fig. 7.** Effective back surface recombination velocity ( $S$ ) as a function of the width ( $W_n^+$ ) of the heavily doped region.

#### 4. Conclusion

In this paper an analytical study has been carried out on the injected dark current of a  $p^+n$  junction solar cell and a  $p^+n^+n^+$  BSF cell taking into consideration heavy doping effect. At heavy doping, band gap narrowing takes place in the semiconductor. The results obtained show that there is significant increase in the value of injected dark current of a solar cell when the band gap narrowing effect is taken into account. Also, the magnitude of the injected dark current decreases for smaller values of back surface recombination velocity, which corresponds to a BSF structure. The  $p^+n^+n^+$  BSF solar cell, therefore, gives better performance over the conventional  $p^+n$  cell, because of the larger values of short circuit current and smaller dark current. It may be mentioned here that earlier studies on  $n^+p-p^+$  BSF solar cells have shown that the open circuit voltage and efficiency of these BSF cells are much higher than the conventional  $n^+p$  junction solar cells. This has been attributed to the larger short circuit current and smaller dark current of the BSF solar cells [11]. Therefore, work done in this paper for a  $p^+n^+n^+$  BSF solar cell is in agreement with the research work reported earlier by several researchers for an  $n^+p^+n^+$  BSF solar cell.

#### Acknowledgements

We are grateful to the Department of Science and Technology, Govt. of India, for financial support granted to the University of Kalyani, under the DST-PURSE programme. We thank the authorities of the Indian Association for the Cultivation of Science, Kolkata, India, for allowing us to consult their library.

**References**

- [1] D.M. Chapin, C.S. Fuller and G.L. Pearson, "A new silicon p-n junction photocell for converting solar radiation into electrical power". *J. Appl. Phys.* vol. 25, pp. 676 - 677, May (1954).
- [2] A.W. Blakers and M.A. Green, "20% efficiency silicon solar cells", *Appl. Phys. Lett.*, vol. 48, pp. 215-217, Jan 1986.
- [3] W. Wang, J. Zhao and M.A. Green, "24% efficiency silicon solar cells", *Appl. Phys. Lett.* vol. 57, pp. 602-604, August 1990.
- [4] Godlewski M.P., Baraona C.R., and Brandhorst H.W., Jr., "The drift field model applied to the lithium-containing silicon solar cell", *Conf. Rec. IEEE Photo. Spec. Conf.*, 10<sup>th</sup> Palo Alto, pp. 40, 1973.
- [5] V. Perraki, "Modeling of recombination velocity and doping influence in epitaxial silicon solar cells", *Solar Energy Materials and Solar Cells*, vol. 94, pp. 1597-1603, June 2010.
- [6] J. Mandelkorn and J.L. Lamneck, "A new electric field effect in silicon solar cell", *J. Appl. Phys.* vol. 44, pp 4785-4787, 1973.
- [7] J.G. Fossum and E.L. Burgeess, "High efficiency p<sup>+</sup>n n<sup>+</sup> back-surface-field silicon solar cells" *Appl. Phys. Lett.*, vol. 33(3) pp. 238-240, 1978.
- [8] H.T. Weaver and R.D. Nasby, "Analysis of high efficiency silicon solar cells *IEEE Trans. On Electron devices*, vol. ED-28, No. 5, pp. 465-472, 1981.
- [9] A. Silard et al., "High efficiency large area p<sup>+</sup> n n<sup>+</sup> silicon solar cells", *Solid State Electronics*, vol. 30, No. 4 pp. 397-401, 1987.
- [10] A.K. Biswas et al., "Analysis of the p<sup>+</sup> n n<sup>+</sup> Back Surface Field Silicon Solar Cell and its Comparison with the Conventional p<sup>+</sup> n Structure", *IJAER*, vol. 10, No. 13, pp. 33025-33028, 2015.
- [11] H. J. Hovel, *Semiconductors and Semimetals*, vol.11, Solar cells, Academic Press, New York, 1975, pp. 49-53 and pp. 24.
- [12] A. Ibrahim, "Dark current-Voltage characteristics and Lock-in Thermography Technique as Diagnostic Tools for Monocrystalline Silicon Solar cells", *IJRER*, vol. 1, No. 3, pp. 60-65, 2011.
- [13] J. W. Slotboom, "The pn - product in silicon", *Solid State Electronics*, vol. 20, pp. 279-283, 1977.
- [14] Slotboom and H.C. De Graaff, "Measurements of Band gap Narrowing in Si Bipolar Transistors", *Solid- State Electronics*, vol. 19, pp. 857-862, 22 March, 1976.
- [15] A. Sinha and S. K. Chattopadhyaya, "Effect of heavy doping on the properties of high-low junction", *IEEE Transactions on Electron Devices*, vol. 25, pp. 1412-1414, 1978.
- [16] A. Sinha and S.K. Chattopadhyaya, "Effect of back surface field on photocurrent in a semiconductor junction", *Solid State Electronics*, vol. 21, pp. 943-951, 1978.
- [17] A. W. Wider, *IEEE, Trans. Electron Dev*, Ed-27 pp. 1402, 1980.
- [18] S. M. Sze and K. K. Ng, *Physics of Semiconductor devices*, John Wiley & Sons, 2007, pp. 80-83.
- [19] D.M. Caughey and R.E. Thomas, "Carrier mobilities in silicon empirically related to doping and field", *Proc. IEEE*, vol.55, pp. 2192 - 2193, Dec. 1967.
- [20] J. G. Fossum, "Computer aided numerical analysis of silicon solar cells", *Solid State Electronics*, vol. 19, pp. 269 - 277, April 1976.